Published in final edited form as:
Inf Process Med Imaging. 2011 ; 22: 320–332.

White Matter Bundle Registration and Population Analysis Based on Gaussian Processes

Demian Wassermann[1,2,3], **Yogesh Rathi**[2], **Sylvain Bouix**[2], **Marek Kubicki**[2], **Ron Kikinis**[3], **Martha Shenton**[2], and **Carl-Fredrik Westin**[1]

[1]Laboratory of Mathematics in Imaging, Brigham & Women's Hospital, Boston, MA

[2]Psychiatry and Neuroimaging Lab, Brigham & Women's Hospital, Boston, MA

[3]Surgical Planning Lab, Brigham & Women's Hospital, Boston, MA

Abstract

This paper proposes a method for the registration of white matter tract bundles traced from diffusion images and its extension to atlas generation. Our framework is based on a Gaussian process representation of tract density maps. Such a representation avoids the need for point-to-point correspondences, is robust to tract interruptions and reconnections and seamlessly handles the comparison and combination of white matter tract bundles. Moreover, being a parametric model, this approach has the potential to be defined in the Gaussian processes' parameter space, without the need for resampling the fiber bundles during the registration process. We use the similarity measure of our Gaussian process framework, which is in fact an inner product, to drive a diffeomorphic registration algorithm between two sets of homologous bundles which is not biased by point-to-point correspondences or the parametrization of the tracts. We estimate a dense deformation of the underlying white matter using the bundles as anatomical landmarks and obtain a population atlas of those fiber bundles. Finally we test our results in several different bundles obtained from in-vivo data.

Keywords

Diffusion MRI; White Matter Fiber Tracts; Gaussian Processes; Registration

1 Introduction

The analysis of inter-population brain variability through imaging is an area of extensive study. Within this area, generating a common coordinate space for analyzing several subjects is one of the main issues to be solved. The development of algorithms capable of registering scalar images, like those obtained from anatomical MRI, and volumes, like sub-cortical structures such as the hippocampus, yielded several effective techniques which enabled a wide range of statistical studies. However, existing tools for the registration of curve sets, such as white matter tract bundles obtained from diffusion MRI (dMRI), are still in need of development.

Current approaches to the registration of cerebral white matter tract bundles can be divided in two families: indirect and direct algorithms. The family of indirect methods starts by performing a full-brain registration. Then, the tract bundles are warped using the resulting deformation field obtained from this registration process. These methods use scalar images like the fractional anisotropy (FA) to obtain the deformation fields [18, 10]. A second set of

methods within this family use directional information, such as the principal diffusion direction of the estimated tensors, to obtain the displacement vectors [22, 21, 6]. There are two main issues with this kind of registration when applied to the warping of tracts bundles. First, the continuity of tracts is not explicitly enforced resulting in tracts being cut or warped into unusual shapes. Second, if the continuity is enforced at a voxel (or supra voxel) level, the directional uncertainties within these voxels, produced by partial voluming or limitations of the diffusivity model will lead to a predominance of the most voluminous tracts, like the corona radiata, sectioning or eliminating the small ones like short cortico-cortical fasciculi.

The family of direct methods registers the tracts explicitly. Of these methods, some algorithms require fiber-to-fiber and point-to-point matching between the tracts [16, 8]. These approaches are subject to tractography artifacts like discontinuities on tracts and parametrization differences. Other methods register volumetric representations of tracts. Ziyan et al. [23] model the white matter bundles as a voxelized mixture of spatial density functions, bounding his approach to an explicit resolution. Moreover, while registering several clusters of tracts, they only account for an affine transformation per cluster considering each cluster as a geometrical landmark to be affinely registered. This does not account for anatomical variability as in several cases, like uncinate fasciculi, the shape of the tract is largely variable between subjects [15]. Durrleman et al. [9] propose a sound diffeomorphic approach based on currents and LLDDM registration [5] and they incorporate a statistical analysis model. However, their approach strongly relies on the orientation of the tract parametrization. This notion of orientation introduced in their distance metric imposes a constraint to the model which is artefactual: diffusion imaging does not provide information about the orientation of the tracts, only their direction. It is not possible to distinguish between the case of an axonal package going from A to B or from B to A. Hence, it is not possible to calculate the orientation of the tracts, the need for an orientation [9] requires the user to reorient all the tracts to be registered consistently, a task which is not at all trivial.

In this work we propose a new approach to the direct diffeomorphic registration of white matter bundles. Our method has four main advantages: we register tract bundles directly; it does not rely on point-to-point nor fiber-to-fiber correspondences as [16, 8]; it is not sensitive to inter-subject total density variations; and it does not depend on the fiber parametrization as [9]. We start by representing the white matter tracts as Gaussian processes (GPs) [20]. This representation associates each tract and each bundle of tracts with a GP mapping each point in space to the density of tracts crossing that point, a tract density map (TDM). It provides a framework where the similarity between two bundles is measured in terms of the mass of common density areas. This metric does not depend on point-to-point correspondences nor on the orientation of the tract parametrization. Moreover, it is calculated from the parameters of the GP without the need for explicit sampling the TDM. We use this similarity to derive a diffeomorphic registration algorithm based on the Log-Euclidean poly-affine framework [3]. Then we use this pairwise registration algorithm along with several desirable properties of our GP framework in order to develop a template estimation algorithm along with a methodology to analyze the characteristic anatomical variations of a population. Finally, we test our algorithms on two different sets of white matter bundles in order illustrate its efficacy.

2 Methods

In this section we introduce our new registration and template estimation methods for white matter bundles. We start by presenting the Gaussian Process-based representation of bundles and their properties which are useful to the development of our algorithms. Then, we develop our registration by using the inner product on our GP-space in combination with a

variant of the polyaffine registration algorithm [3]. Finally, we present our template estimation algorithm based on our pairwise registration method and the work of [2].

2.1 Representation of WM Bundles as Tract Density Maps

As emphasized in [7, 12, 20] a normalized tract density map (TDM) is a convenient non-parametric way to model white matter fiber bundles. For WM tract bundle composed of N tracts, the TDM is a function $y(\mathbf{p}) \triangleq \#t/N$ that associates each point $\mathrm{p} \in \mathbb{R}^3$ with the ratio of number of tracts $\#t$ that are likely to traverse that point over the total number of tracts in the bundle, N. We show examples of TDMs for WM tracts in fig. 1.

In order to calculate TDMs for WM tracts [4], we use a Gaussian Process (GP) framework [20]. The advantages of this representation are three-fold: first, the TDMs calculated using GPs are continuous functions which can be sampled at any desired resolution; second, being a parametric representation, the GP framework allows us to work robustly on its parameter space instead of performing operations in image space; third, this representation provides us with a vector space of TDMs which we use in order to derive a tract registration algorithm. In the remainder of this section we detail the calculation of TDM for a WM tract: we start by describing the representation of a trajectory within the GP framework; next, we show how to go from the GP representation of a single trajectory to the representation of a bundle of trajectories; and finally, using the GP framework, we describe the calculation of the TDM for a bundle of trajectories.

We model the TDM of an individual trajectory $\mathcal{F}$ as a tract density map $y(\cdot)$, such that, for any point $\mathbf{p} \in \mathcal{F}$, $y(\mathbf{p}) = 1$ and it decays to 0 for points far away from $\mathcal{F}$ at a speed modulated by a parameter R. This smooth TDM $y(.)$ of a single trajectory $\mathcal{F}$ can be written as a GP, $y \tilde{\mathcal{GP}}(y^*(\cdot), c(\cdot,\cdot))$, [20] where $y^*(\cdot)$ is the most probable TDM for trajectory $\mathcal{F}$, or $y^*(\cdot) = \mathbb{E}\{y(\cdot)\}$ and $c(\cdot, \cdot)$ is derived from the hypotheses on the shape and smoothness of the TDM and characterizes the variability of suitable TDMs for $\mathcal{F}$. Then, using the properties of the GPs, the value of $y(\cdot)$ for a trajectory can be characterized at each point in space $\mathbf{p}$ as an univariate Gaussian: $y(\mathbf{p}) \tilde{\mathcal{G}}\left(y^*(\mathbf{p}), \sigma^2(\mathbf{p})\right)$. Particularly, sampling a set of points $\mathbf{f} = \{\mathbf{f}_1, \ldots, \mathbf{f}_N\}$ from the trajectory $\mathcal{F}$, the mean and the variance of this univariate Gaussian are inferred as

$$y^*(\mathbf{p}) = [C_{\mathbf{f}}(\mathbf{p})]^T C_{\mathbf{ff}}^{-1} 1 \quad \text{and} \quad \sigma^2(\mathbf{p}) = c(\mathbf{p},\mathbf{p}) - C_{\mathbf{f}}(\mathbf{p})^T C_{\mathbf{ff}}^{-1} C_{\mathbf{f}}(\mathbf{p}) \tag{1}$$

where

$$[C_{\mathbf{f}}(\mathbf{p})]_i \triangleq [c(\mathbf{f}_i, \mathbf{p})]_i, \qquad [C_{\mathbf{ff}}]_{ij} \triangleq \left[c\left(\mathbf{f}_i, \mathbf{f}_j\right)\right]_{ij}, \qquad 1 = [1 \ldots 1]^T$$

and

$$c\left(\mathbf{p}, \mathbf{p}'\right) \triangleq \psi\left(\| \mathbf{p} - \mathbf{p}' \|\right), \qquad \psi(r) = \begin{cases} 2|r|^3 - 3Rr^2 + R^3 & r \le R \\ 0 & r > R \end{cases}.$$

The covariance function used to characterize this GP, $c(\cdot, \cdot)$, has two important properties [20]: first, it ensures that the most probable TDM representing a given fiber minimizes the curvature; second, the resulting TDM has finite support of radius R around each point[4]. Later, we will take advantage of the finite support property to specify a finite block coverage of the TDM.

This GP framework constitutes a **vector space** where $(y_1+y_2)(\mathbf{p}) = y_1(\mathbf{p})+y_2(\mathbf{p})$ and $(\lambda y_1)(\mathbf{p}) = \lambda y_1(\mathbf{p})$. Using these operations, obtaining the representation for a bundle of trajectories $\mathcal{B}= \{\mathcal{F}_1, \ldots, \mathcal{F}_N\}$ is straightforward: we calculate the mean y^* and variance σ of the Gaussian distribution characterizing the TDM for the bundle $\mathcal{B}$ at a point $\mathbf{p}$ as [20]

$$y^*_{\mathcal{B}}(\mathbf{p}) = \frac{1}{N}\sum_{\mathcal{F}\in\mathcal{B}} y^*_{\mathcal{F}}(\mathbf{p}) \qquad \text{and} \qquad \sigma_{\mathcal{B}}(\mathbf{p}) = \frac{1}{N^2}\sum_{\mathcal{F}\in\mathcal{B}} \sigma^2_{\mathcal{F}}(\mathbf{p}).$$

The result of the combination of the density functions representing various trajectories into a bundle is illustrated in fig. 2(e).

We quantify the similarity between two WM bundles by using the deterministic *inner product* of this vector space,

$$\langle y_1, y_2\rangle = \mathbb{E}\left\{\int_{\mathbb{R}^3} y_1(\mathbf{p})\, y_2(\mathbf{p})\, d\mathbf{p}\right\} = \int_{\mathbb{R}^3} y_2^*(\mathbf{p})\, y_2^*(\mathbf{p})\, d\mathbf{p} \tag{2}$$

which represents the overlap between the TDMs of the two tracts. Using eq. (1), we calculate $\langle y_1 , y_2\rangle$ without point-to-point matching between bundles [20]

$$\langle y_1, y_2\rangle = 1^T \left[C^{-1}_{\mathbf{f}^1\mathbf{f}^1}\right]^T \left(\int_{\mathbb{R}^3} C_{\mathbf{f}^1}(\mathbf{p})\left[C_{\mathbf{f}^2}(\mathbf{p})\right]^T d\mathbf{p}\right) C^{-1}_{\mathbf{f}^2\mathbf{f}^2} 1 \tag{3}$$

where $\mathbf{f}^1$ and $\mathbf{f}^2$ are the points of to the two bundles. Also, $\langle ., .\rangle$ induces the norm $\|y\|^2 = \langle y, y\rangle$ representing the mass of the tract. Current literature in Gaussian processes [1, 14] shows that the **inner product space** we just presented is, in fact, a **reproducible kernel Hilbert space** (RKHS), allowing to define a set of basis functions whose linear combination spans all TDMs. Later in this paper, we use this RKHS property to characterize the deformation modes of a particular population of WM tracts.

In the above, we have presented a GP-based framework for representing white matter fiber bundles and three operations: the calculation of the normalized tract density map, combination of fibers into a bundle and the quantification of the similarity between two bundles. These tools are fundamental to performing white matter bundle registration, which we develop in the next section.

2.2 Diffeomorphic Bundle Registration with GP-represented TDMs

Our goal is to align two WM bundles obtained from two different subjects. In other words, given the two bundles $\mathcal{B}_1, \mathcal{B}_2$ and their corresponding GP-represented TDMs y_1, y_2, we are looking for a dense transformation $s : \mathbf{p} \mapsto \mathbf{s}(\mathbf{p})$ such that it minimizes

$$E(s) = \text{Sim}(s) + \text{Reg}(s) \quad \text{where} \quad \text{Sim}(s) = 1 - \frac{\langle y_1, y_2 \circ s\rangle^2}{\| y_1 \| \| y_2 \circ s \|} \tag{4}$$

where Sim(s) is the TDM similarity measure and Reg(s) is a regularization term. In this equation, the transport of the TDM y_2 by the transformation s, $y_2 \circ s$, is carried by the operation $(y_2 \circ s)(\mathbf{p}) = y_2(\mathbf{s}(\mathbf{p}))\ \text{jac}\ \mathbf{s}(\mathbf{p})|$. Equation (4) can be regarded as equivalent

[4] We take as 2 times the maximum distance between two consecutive points in the tract.

minimizing the widely used normalized cross-correlation metric [11] between the images of two TDMs.

In order to develop a diffeomorphic registration algorithm with a reduced number of parameters, we use a variant of the LogEuclidean polyaffine technique [3] to minimize eq. (4) and obtain the desired registration. We start by dividing the domain of y_1, y_2 in a lattice of cubic blocks of volume W. Since y_1 and y_2 are of finite support (section 2.1), it is possible to define a finite set Γ of non-intersecting blocks of volume W which is a total coverage of the two TDMs: $\Gamma = \{\gamma_1, \ldots, \gamma_N\} \subset \mathbb{R}^3$. Figure 3(a) illustrates a TDM along with its lattice Γ. Using this set, we define a block-based registration energy which is an upper bound approximation for eq. (4) as

$$\mathbb{E}_\Gamma(s) = \mathrm{Sim}_\Gamma(s) + \mathrm{Reg}(s), \qquad \mathrm{Sim}_\Gamma(s) = \sum_{i=1\ldots N} 1 - \frac{\langle y_1, y_2 \circ s \rangle^2_{\gamma_i}}{\| y_1 \|_{\gamma_i} \| y_2 \circ s \|_{\gamma_i}} \tag{5}$$

where we define the block-inner product and its induced norm as

$$\langle y_1, y_2 \rangle_\gamma \triangleq \int_\gamma y_1^*(\mathbf{p})\, y_2^*(\mathbf{p})\, d\mathbf{p}, \qquad \| y \|^2_\gamma = \langle y, y \rangle_\gamma. \tag{6}$$

The block-based formulation of the registration energy, eq. (5), enables us solve our registration problem using a block-based polyaffine framework. Let M and $\mathbf{t}$ be the linear and translation components of the affine transform A. Defining the affine transformation of a TDM $(y_2 \circ A) \triangleq y_2(M \cdot \mathbf{p} + \mathbf{t})$ renders possible to obtain an affine registration inside of the block γ by minimizing

$$A_\gamma = \mathrm{argmin}'_A \left\{ 1 - \frac{\langle y_1, y_2 \circ A' \rangle^2_\gamma}{\| y_1 \|_\gamma \| y_2 \circ A' \|_\gamma} \right\} \tag{7}$$

Then, using the LogEuclidean polyaffine framework [3] we calculate the dense diffeomorphic transform s from a set of affine transforms: we compute the velocity field u associated with the affine transforms $A_{\gamma 1}, \ldots, A_{\gamma N}$, as

$$u: \mathbf{p} \mapsto \mathbf{u}(\mathbf{p}), \qquad \mathbf{u}(\mathbf{p}) = \sum_{i=1\ldots N} w_{\gamma i}(\mathbf{p}) \left(L_{\gamma i} \mathbf{p} + \mathbf{v}_{\gamma i} \right), \tag{8}$$

where

$$\begin{pmatrix} L_\gamma & V_\gamma \\ 0 & 0 \end{pmatrix} = \log\left(A_\gamma\right). \qquad L_\gamma \in \mathbb{R}^{3\times 3}, \mathbf{v}_\gamma \in \mathbb{R}^3,$$

and $w_\gamma(\mathbf{p})$ is a smooth weighting function which quantifies the influence that the transform found at block γ has on $\mathbf{p}$ and log is the matrix logarithm. Particularly, we define

$$w_\gamma(\mathbf{p}) = \frac{w'_\gamma(\mathbf{p})}{\Sigma_{\gamma \in \Gamma} w'_\gamma}, \qquad w'_\gamma(\mathbf{p}) = \exp\left(- \frac{\| \mathbf{p} - \bar{\gamma} \|^2}{\sigma^2} \right)$$

where $\bar{\gamma}$ is the center of block γ and σ controls the rigidity of the global transformation.

We can now present our TDM-based polyaffine white matter bundle registration algorithm: Given two white matter bundles as their TDMs, y_1, y_2 and a block volume W,

1. Calculate the non intersecting block-coverage of y_1 and y_2: $\Gamma = \{\gamma_1, \cdots, \gamma_N\}$
2. Set the initial transform $s_0 = Id$
3. **repeat**
4. $s_{prev} \leftarrow s$
5. Find the set of affine transforms $A_{\gamma i}$, $i = 1 \ldots N$, minimizing $\mathrm{Sim}_\Gamma(s_k)$ (eq. (5))
6. Calculate the velocity field u using eq. (8)
7. Compose the transforms $c \leftarrow s_{prev} \circ \exp(u)$
8. For a diffusion-like regularization $s \leftarrow K_{diff} \star c$, else $s \leftarrow c$
9. **until** $E_\Gamma(s_{prev}) - E_\Gamma(s) <$ threshold

where exp is the exponential of a vector field as defined by [3] and $K_{diff} \star c$ is the convolution of the velocity field c with the Gaussian kernel K_{diff}. Figure 3 depicts a step of the algorithm presented above. Two things should be noted in this algorithm: first, we are using a two-step optimization process as in Vercauteren et al [19]; second, we want to highlight that a multiscale version of this algorithm is easily implementable by adding an outer loop which varies the volume of the blocks in a monotonic decreasing manner.

2.3 Template Construction and Population Analysis

We now extend our pairwise registration algorithm to groupwise registration in order to generate an unbiased template[13, 2].

We consider having M analogous bundles $\mathcal{B}_1, \ldots, \mathcal{B}_M$ extracted from rigidly co-registered images of M subjects. Following Allassonniere [2] and Durrleman [9], we consider the bundles the result of a diffeomorphic deformation of a prototype bundle plus a residual. Letting y_i be the GP-based TDM representation associated with bundle $\mathcal{B}_i$, we formulate the TDM of each bundle in terms of the template as

$$y_i(\mathrm{p}) = \left(\bar{y} \circ s_i\right)(\mathrm{p}) + \epsilon_i(\mathbf{p}), \qquad \mathrm{p} \in \mathbb{R}^3$$

where $\omega_i(\mathbf{p})$ is an image of uncorrelated white noise represented by a zero mean Gaussian process with diagonal covariance function, $c_\omega(\mathbf{p}, \mathbf{p}') = \delta(\|\mathbf{p} - \mathbf{p}'\|)$, where $\delta(\cdot)$ is the Dirac delta function. This covariance function stands for absence of correlation between the points in the image or white noise. Then we estimate the template, the deformations and the residues as:

$$\mathrm{argmin}_{\bar{y}, s_i} \left\{ \sum_{i=1}^{M} \mathrm{Sim}_\Gamma\left(y_i, \bar{y} \circ s_i\right) + Reg(S_i) \right\} \tag{9}$$

We minimize the criterion in eq. (9) using alternate minimization: initially we set $s_i = Id$ and we obtain a first estimate of the template $\bar{y} = \sum_i y_i / M$; then we register $\bar{y}$ to every bundle y_i,

and we re-estimate the template $\bar{y} = \sum_i \left(y_i \circ s_i^{-1} \right) / M$; finally, we iterate these steps until convergence.

This algorithm eventually yields an unbiased template $\bar{y}$ and the deformations s_i. Taking advantage of the RKHS property of the TDMs y_i and its residuals ω_i represented as GPs, section 2.1, we perform PCA analysis of the residuals in order to characterize the non-diffeomorphic deformations of each bundle. We start by estimating the residual for each bundle $\mathcal{B}_i$ as $\epsilon_i = y_i - \bar{y} \circ s_i$. Then, we calculate the first mode of residual variations on the template at $\pm\theta$, as $m_\epsilon(\theta) = \bar{y} \pm \theta \sum_i \epsilon_i \mathbf{v}_1$ where $\mathbf{v}_1$ is the eigenvector corresponding to the largest eigenvalue of the covariance matrix $[\langle \omega_i , \omega_j \rangle]_{ij}$ (see example in Results section).

We have formulated the necessary tools to perform pairwise registration between white matter bundles represented as TDMs in the GP space; to estimate a template from a population and to characterize its residual variation modes. Our model represents the bundles in a population as a diffeomorphic deformation of a template plus a non-diffeomorphic residual as done by Durrleman et al [9]. These tools to perform statistical analysis of the WM bundles are not biased by point-to-point or fiber-to-fiber correspondences. In addition, it is not biased by differences in the orientation of fiber parametrizations as [9]. The separation between the diffeomorphic and residual part is regulated by the tradeoff between the similarity between bundles and the regularization term used in order to find the diffeomorphic transforms in eq. (4). This allows to adjust the deformation and to capture subject-specific anatomical variations. We are now in position to apply all these tools to a bundle population and analyze it.

3 Results

Diffusion-weighted images (DWI) from 43 subjects were acquired on a GE Signa HDxt 3.0T scanner using an echo planar imaging sequence with a double echo option, an 8 Channel coil and ASSET with a SENSE-factor of 2. The acquisition consisted in 51 directions with b=900 s/mm^2, and 8 images with b=0 s/mm^2, with scan parameters TR=17000 ms, TE=78 ms, FOV=24 cm, 144×144 encoding steps, 1.7 mm slice thickness. 85 axial slices covering the whole brain were acquired. DWI images were linearly registered. The left uncinate and fronto-occipital fasciculi ROI's were manually drawn by experts using 3D Slicer (www.slicer.org) and fiber tracts were obtained using two-tensor tractography [17].

3.1 Pairwise Registration

In order to test the efficacy of our pairwise registration algorithm, introduce in section 2.2, we randomly picked one sample from each bundle population and registered all others to it. We applied a multiresolution scheme where the cubes of the latices were 100, 50, 20, 10 and 5mm^3 each and we set rigidity parmeter σ to 1/2 of the cube width. For the uncinate fasciculi the dice coefficient of the registered TDMs to the fixed TDM was .93(±03) and for the fronto-occipital bundles .81(±07). We applied the transformation s_i to each moving bundle $\mathcal{B}_i$, and the results for one example of each bundle class are shown in fig. 4. In this figure we show, from left to right, the progress of the registration of two uncinate fasciculi and two fronto-occipital bundles, red indicates the moving bundle and green the fixed one.

3.2 Template Estimation

We applied the template estimation algorithm presented in section 2.3 to both populations of white matter bundles. In fig. 6, we show the convergence of the template estimation algorithm. The algorithm starts from a set of bundles extracted from rigidly registered DT

images and converges to an unbiased template. After the template estimation, we assessed the quality of the results by calculating the Dice coefficient of the population of uncinate fasciculi with the estimated template: 0.97(±0.015); the same analysis for the occipito-frontal dataset had a Dice coefficient of 0.85(±0.075). To compare our approach with indirect image-based registration, we applied the warps generated from a DWI-based template estimation algorithm [6] to the uncinate fasciculi and we compared them with the results of our bundle-based registration. We extracted two bundles and show the results obtained by applying both methods in fig. 5. Then, we calculated the residuals and their variation modes from the template. In fig. 7 we show the first mode of variation for the uncinate bundle.

4 Discussion and Conclusion

In this paper, we introduced a new approach to the direct registration of white matter tract bundles obtained through diffusion MRI tractography. Our method does not rely on point-to-point correspondences nor on the orientation of tract parametrization. Moreover, the GP-based mathematical framework we used enables us to analyze the characteristic deformations of a population. At the heart of our method is the similarity calculation between two bundles which is independent of point-to-point correspondences or orientation of the tract parametrization. Moreover, we parametrically represent these bundles as Gaussian processes, which has several advantages: 1) the similarity is calculated from the parameters of the GP without the need of explicitly sampling the TDM; 2) the **vector space** of GPs enables us to seamlessly combine bundles, in the intrasubject case where single tracts form a fascicle or the intersubject case where several bundles are combined to form a template 3) The **RKHS space** in which these GPs are embedded provides us with the tools to perform population studies such as PCA. All of these advantages led us to a combined registration and template estimation and population analysis framework.

The results on pairwise registration show that our algorithm effectively produces a deformable registration which puts priority in areas of high fiber density allowing sparse radiations to variate between subjects. This characteristic is important as it enables us to achieve a registration on the main trunk of the tract bundle and leave a degree of freedom for inter subject anatomical variations as those shown by Bürgel et al [7]. When we compared the outcome of our template estimation algorithm with a DWI-based one, ours showed a higher overlap in the bundles. Particularly, we illustrated this by extracting two bundles of the population and showing their overlap. The statistical analysis was evaluated on fibers obtained from 43 subjects. The characteristic deformation shows variability in the innervations of the orbital cortex and the temporal pole which is coherent with histological studies [7].

The method however, raises a main question: how much are we losing by not taking explicitly in account the orientation of the tracts. According to the experiments we performed in this paper, our registration algorithm yields good results even in the absence of orientation features in our model. Since our model based on the density of tracts at each point, the continuity of the density map and the diffeomorphic transforms lead to a registration algorithm which results in the alignment of the most dense areas of the tracts. When the tract has several diverging fibers like the occipito-frontal fasciculi these are allowed to vary between subjects and considered by the template estimation algorithm as non-diffeomorphic transforms. Hence, even if orientation information is not taken in account, our algorithm registers the most dense areas of the tracts effectively.

Further work will focus on the development of discriminative statistics and correlation analyses. Discriminative statistics are fundamental when studying pathologies and

comparing populations, the development of a suitable hypothesis testing scheme is then of the utmost importance. Along the same lines, correlation analyses, for instance with scalar indices, will enable to characterize the cognitive or pathological consequences of the anatomical variations unveiled by our population analysis tools.

Acknowledgments

This work was supported by P41RR13218 (RR) funded by NCRR NIH HHS; U41RR019703 (RR) funded by NCRR NIH HHS; U54EB005149 (EB) funded by NIBIB NIH HHS; R01MH5074 funded by NIMH NIH; VA Schizophrenia Center Grant; VA Merit Award; R01MH074794; R01MH092862; 5R01MH82918; and P41RR013218.

References

1. Adler, RJ.; Taylor, JE. Random Fields and their Geometry. Springer; 2007.
2. Allassonnière S, Amit Y, Trouvé A. Towards a coherent statistical framework for dense deformable template estimation. J. of the Royal Stat. Soc.B. 2007; 69(1):3–29.
3. Arsigny V, Commowick O, Ayache N, Pennec X. A fast and log-euclidean polyaffine framework for locally linear registration. JMIV. 2009; 33(2):222–238.
4. Basser P, Pajevic S, Pierpaoli C, Duda J, Aldroubi A. In vivo fiber tractography using DT-MRI data. Magnetic Resonance in Medicine. 2000; 44(4):625–632. [PubMed: 11025519]
5. Beg M, Miller M, Trouvé A, Younes L. Computing large deformation metric mappings via geodesic flows of diffeomorphisms. IJCV. 2005; 61(2):139–157.
6. Bouix, S.; Rathi, Y.; Sabuncu, M. MICCAI Workshop on Computational Diffusion MRI. 2010. Building an average population hardi atlas.
7. Bürgel U, Amunts K, Hoemke L, Mohlberg H, Gilsbach JM, Zilles K. White matter fiber tracts of the human brain: Three-dimensional mapping at microscopic resolution, topography and intersubject variability. NeuroImage. 2006; 29(4):1092–1105. [PubMed: 16236527]
8. Corouge I, Fletcher PT, Joshi S, Gouttard S, Gerig G. Fiber tract-oriented statistics for quantitative diffusion tensor mri analysis. MIA. 2006; 10(5):786–798.
9. Durrleman S, Fillard P, Pennec X, TrouvÈ A, Ayache N. Registration, atlas estimation and variability analysis of white matter fiber bundles modeled as currents. NI. 2010 http://www.sciencedirect.com/science/article/B6WNP-51K9388-1/2/2094f276b437215fa1da04614514f48b.
10. Goodlett CB, Fletcher PT, Gilmore JH, Gerig G. Group analysis of dti fiber tract statistics with application to neurodevelopment. NeuroImage. 2009; 45(1, S1):S133–S142. http://www.sciencedirect.com/science/article/B6WNP-4TXF7Y2-3/2/63144928840f25440fbdfac042c2b2b4. [PubMed: 19059345]
11. Holden M. A review of geometric transformations for nonrigid body registration. TMI. 2008; 27(1):111–128.
12. Hua K, Zhang J, Wakana S, Jiang H, Li X, Reich DS, Calabresi PA, Pekar JJ, van Zijl PCM, Mori S. Tract probability maps in stereotaxic spaces: Analyses of white matter anatomy and tract-specific quantification. NeuroImage. 2008; 39(1):336–347. http://www.sciencedirect.com/science?_ob=MImg&_imagekey=B6WNP-4PF1WFR-5-N&_cdi=6968&_user=6068170&_orig=search&_coverDate=01%2F01%2F2008&_sk=999609998&view=c&wchp=dGLbVlz-zSkzS&md5=de42ccbb978bccd0c2bf38c987ee787e&ie=/sdarticle.pdf. [PubMed: 17931890]
13. Joshi S, Davis B, Jomier M, Gerig G. Unbiased diffeomorphic atlas construction for computational anatomy. NeuroImage. 2004; 23(S1):S151–S160. http://www.sciencedirect.com/science/article/B6WNP-4DCMGVT-3/2/77a14449f2c349bbfc9c36758645eaac. [PubMed: 15501084]
14. Kimeldorf G, Wahba G. A correspondence between Bayesian estimation on stochastic processes and smoothing by splines. Ann. of Math. Stat. 1970; 41(2):495–502.
15. Kubicki M, Westin C, Maier S, Frumin M, Nestor P, Salisbury D, Kikinis R, Jolesz F, McCarley R, Shenton M. Uncinate Fasciculus Findings in Schizophrenia: A Magnetic Resonance Diffusion Tensor Imaging Study. American J Psychiatry. 2002; 159(5):813.

16. Leemans A, Sijbers J, Backer SD, Vandervliet E, Parizel P. Multiscale white matter fiber tract coregistration: a new feature-based approach to align diffusion tensor data. MRM. Jun; 2006 55(6):1414–1423. http://dx.doi.org/10.1002/mrm.20898.

17. Malcolm JG, Michailovich O, Bouix S, Westin CF, Shenton ME, Rathi Y. A filtered approach to neural tractography using the Watson directional function. MIA. 2010; 14:58–69.

18. Smith SM, Jenkinson M, Johansen-Berg H, Rueckert D, Nichols TE, Mackay CE, Watkins KE, Ciccarelli O, Cader MZ, Matthews PM, Behrens TEJ. Tract-based spatial statistics: voxelwise analysis of multi-subject diffusion data. NI. 2006; 31(4):1487–1505. http://dx.doi.org/10.1016/j.neuroimage.2006.02.024.

19. Vercauteren T, Pennec X, Perchant A, Ayache N. Diffeomorphic demons: Efficient non-parametric image registration. NeuroImage. 2009; 45(1, S1):S61–S72. http://www.sciencedirect.com/science/article/B6WNP-4TW13J3-6/2/519213aac5e0b363bd17fbd0a05e1833. [PubMed: 19041946]

20. Wassermann D, Bloy L, Kanterakis E, Verma R, Deriche R. Unsupervised white matter fiber clustering and tract probability map generation: Applications of a gaussian process framework for white matter fibers. NeuroImage. 2010; 51(1):228–241. http://www.sciencedirect.com/science/article/B6WNP-4Y5BMD4-2/2/9bba3c64a0443363022999aa7b04918a. [PubMed: 20079439]

21. Yang, J.; Shen, D.; Davatzikos, C.; Verma, R. MICCAI. LNCS; 2008. Diffusion Tensor Image Registration Using Tensor Geometry and Orientation Features; p. 905-913.

22. Zhang H, Yushkevich P, Alexander D, Gee J. Deformable registration of diffusion tensor MR images with explicit orientation optimization. MIA. 2006; 10:764–785.

23. Ziyan, U.; Sabuncu, MR.; Grimson, WEL.; Westin, CF. IEEE MMBIA. 2007. A robust algorithm for fiberbundle atlas construction.

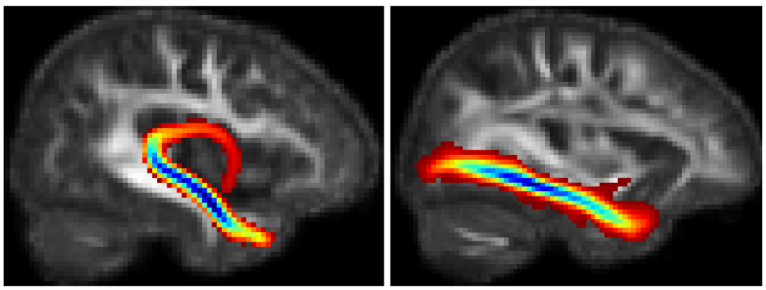

Fig. 1.
Tract density map for the fornix and inferio-longitudinal fasiculus. The density scales from blue (maximum density) to red (minimum density).

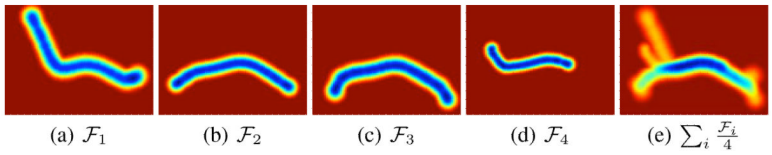

Fig. 2.

Tract density map for four fiber tracts (a-d) and for the bundle formed by averaging them according to our framework (e). Color code ranges from blue when it is likely that a voxel belongs to the bundle of fibres to red when it does not belong. Image reproduced from [20].

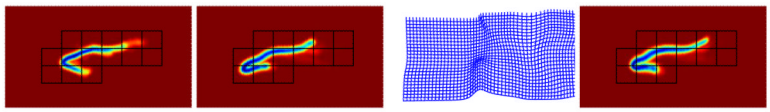

(a) Fixed TDM (b) Moving TDM (c) Deformation (d) Deformed moving TDM

Fig. 3.

Illustration of a registration step. Figures (a-b) show the TDMs corresponding to 2 uncinate fasciculi along with their common lattice Γ, each square indicates a block γ_i. We calculate the affine transforms to take each block of the moving image to the fixed one and integrate them into a deformation (c). Finally, the deformation is applied to the moving image (d).

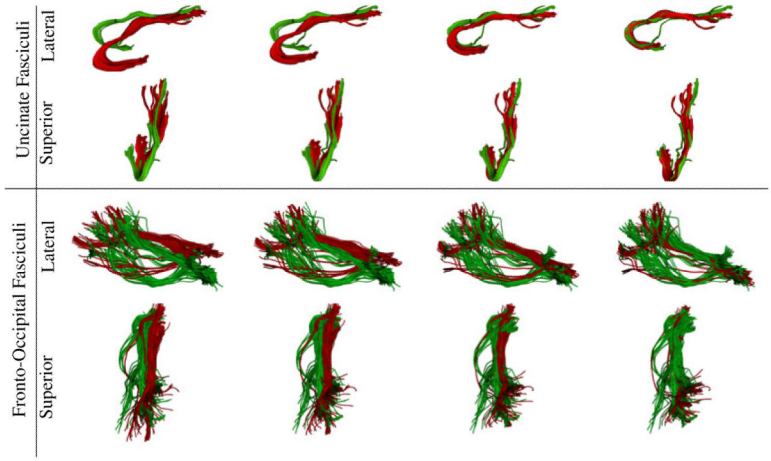

Fig. 4.
Result of the pairwise registration of two uncinate fasciculi and two fronto-occipital bundles. Green indicates the fixed bundle and red the moving one. The registration progress is shown from left two right

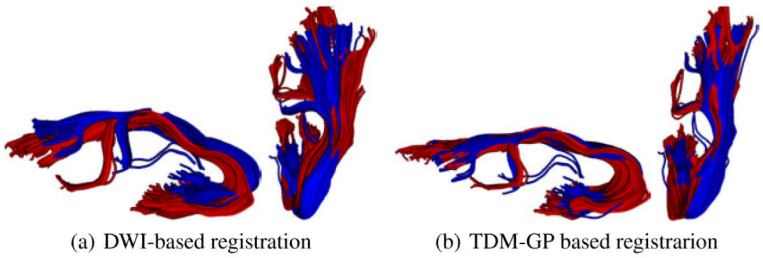

Fig. 5.

Comparison of registration methods: two uncinate fasciculi after volumetric registration their DWI images with a state-of-the-art method [6]: (a) and after applying our bundle-based registration (b) . Overlap is better using our TDM-GP approach than by registering the DWI images.

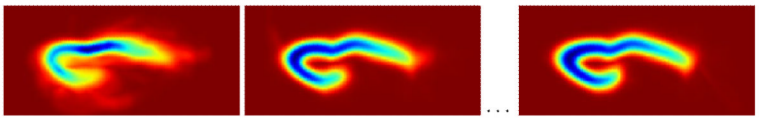

Fig. 6.
Template estimation: several steps of the template estimation algorithm presented in section 2.3. The iterations start from a template generated by linear registartion of the DWI images and converge to unbiased template generated by our algorithm.

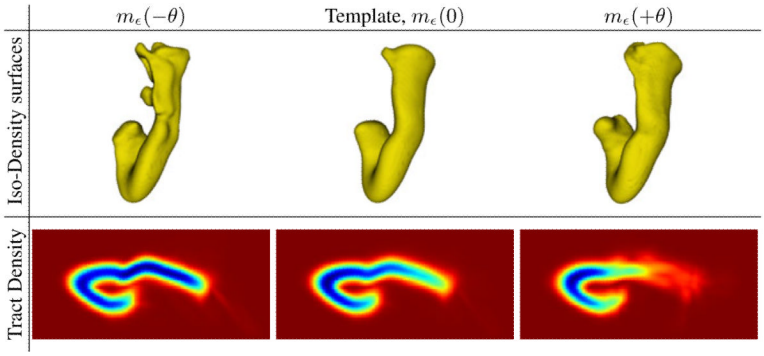

Fig. 7.

First mode of the residual variations on the template. We show the mode on the range $-\theta \ldots \theta$ where 0 is the actual template. We show the iso-density level at 0.01 from a superior point of view on the top and the maximum intensity projection from a lateral point of view on the bottom. The first mode of variation shows a dispersion on the innervations of the uncinate fasciculus at the orbital cortex and the temporal pole.